ASSESSMENT OF BLASTING OPERATIONS EFFECTS DURING HIGHWAY TUNNEL CONSTRUCTION

*Veronika Valašková, Daniel Papán, Marián Drusa**
**Faculty of Civil Engineering, Department of Structural Mechanics, University of Žilina,*
Univerzitná 8214/1, Žilina 010 26, Slovakia
e-mail: drusa@fstav.uniza.sk

Abstract:

Blasting operations are one of the fundamental parts of daily civil engineering. Drilling and blasting still remain the only possible ways of tunnelling in very adverse geological conditions. However, this method is a source of various disadvantages, the main one being tremors propagating through the geological environment which not only affect buildings, but also disturb the comfort of living in the vicinity of the source. Designing this procedure is mostly done using standardized empirical relations. This article shows the possibility of using a FEM technique in predicting blast effects. This approach is demonstrated in a simple case study on the impact of blasting operations on steel pipes.

Keywords: vibration, blasting, FEM simulation, vibration velocity

1 INTRODUCTION

The purpose of this article is to assess the impact of blasting operations during the construction of the Považský Chlmec tunnel on a steel water pipeline, DN 300. This water pipeline is important for supplying the population of the Žilina region with drinking water. The boundary of excavation of the tunnel from this important pipeline, where the usage of blasting operations is a necessity, lies in the nearest spatial perpendicular distance of 8 m from the south tunnel tube and 4 m from the north tunnel tube. The pipeline location towards the central portal part of the tunnel and the direction of the tunnel tubes is shown in Fig. 1. The central portal zone is located in the middle part of the tunnel and was opened for technological reasons (to speed up tunnelling); it is a place where the excavation works are carried out from six tunnel faces simultaneously. Once the highway is completed, it will reduce the heavy traffic on the existing sections of the roads I/11 and I/18. By diverting the traffic outside the town of Žilina, travelling from north to south, both on the national and international highway networks, will become smoother and faster and the economic potential of the Kysuce region will be enhanced. The tunnel is constructed on the section Žilina, Strážov – Žilina, Brodno. The tunnel consists of two 2-lane tunnel tubes 2.2 km long.

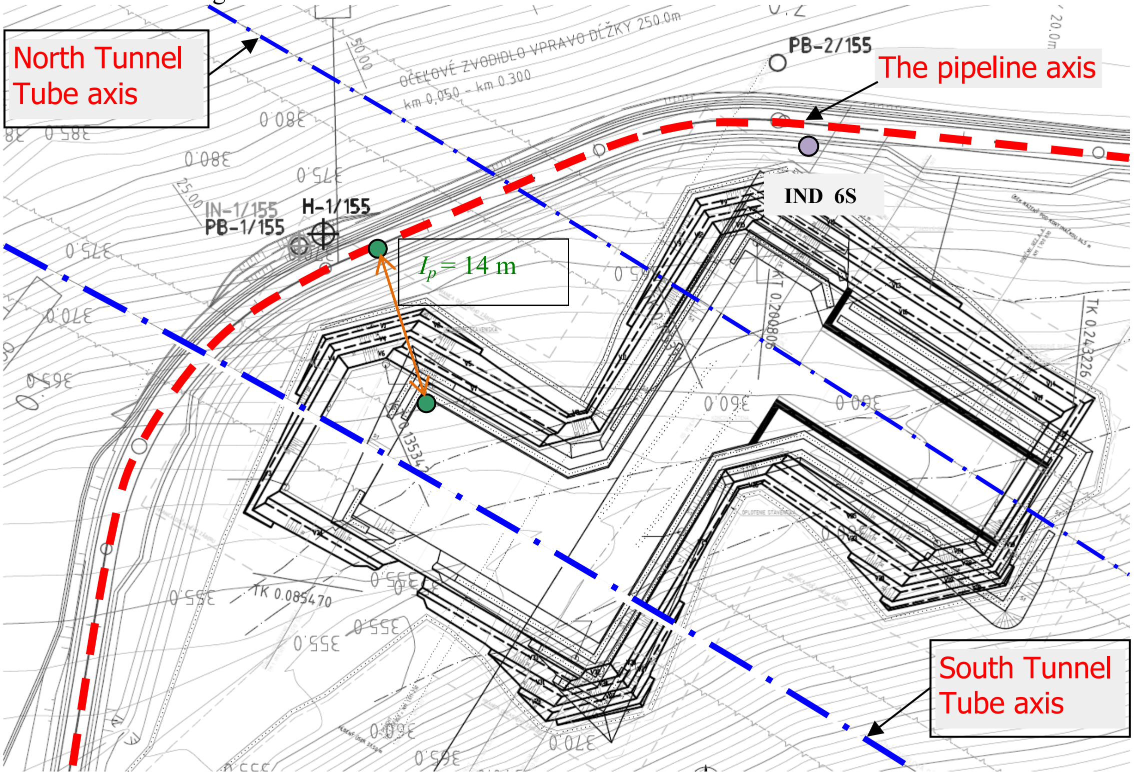

Figure 1: Location of water supply pipeline and open pit construction of central portal zone.

The territory along the tunnel is part of the Outer Carpathian Klippen zone, Kysucko-Pieninská part. The northern and southern parts of the tunnel corridor are formed by flysch formations of calcareous sandstones and mudstones. In the upper strata there are exotic conglomerates and sandstones which are dominated by the layers of marlstones and claystones. In terms of tectonics, the tunnel is located on the eastern edge of the zone of parallel faults oriented N-S known as the Žilina system. Superficial deposits are formed by a deluvial complex of quaternary sediments developed on the slopes of the valley, but also on the top part of the territory of the tunnel [1]. The geological profile in the studied place can be interpreted by the drilled borehole IND_6S shown in Fig. 2.

2 SEISMIC EFFECTS OF BLASTING OPERATIONS

The shock intensity is proportional to parameters such as weight, density and brisance of the applied blasting explosives. Part of the explosion energy, which is not used for intended rock disintegration, penetrates the surrounding environment as a shock pulse. This shock pulse spreads from the point of detonation in all directions in various types of elastic shock waves [2, 3 and 4]. The surface Rayleigh waves (longitudinal and vertical) and Love waves (horizontal) are the most important ones. The propagation velocity of body waves, either of longitudinal P-waves or transverse S-waves, is equal to the speed of sound in the given environment. The characteristic physical quantities of each wave (harmonic motion) are: the amplitude and the frequency of the wave.

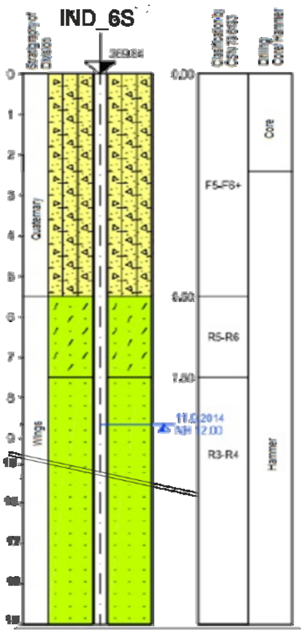

Depth [m]	Geological description
5.50	Clay and silty clay, sandy might not be weak, brown, stiff, moist, with varying representation of fragments and stones greywacke sandstones and conglomerates (size 1-16 cm, content 20-40%), above the weak humous, F5-F6 + cb .... deluvial sediments above pedogen recast
7.50	Eluvium sandstone, among the characteristic rock fragments strength of R4-R3 also present clay fraction coloring drilling output to now, it can be assumed that the position will have lower overall strength in the order of R5-R6 .... eluvium sandstone
18.00	Small thick calcareous sandstones in alternation with the claystone to siltstones, drilling output dark gray, in the interval from 11.5 to 12.5 m. Drilling output colored brown, strength R3-R4

Figure 2: Geological profile along the nearest borehole [1].

Vibrations caused by the explosion of explosive materials are aperiodic and are characterized by their high amplitude and energy. In many cases, the propagation of seismic waves is affected by the surrounding environment which often cannot be precisely defined. Vibrations of the environment caused by an explosion have a similar character as those of a nearby earthquake.

Common frequencies caused by explosive agents are between 5 and 50 Hz. The frequency $f > 10$ Hz corresponds to the charges with an equivalent mass $m_{ev} > 2000$ kg, while the frequency $f > 50$ Hz corresponds to the charges with an equivalent mass $m_{ev} < 5$ kg.

3 CALCULATION OF RESPONSE TO FEM MODEL

3.1 FEM principle for dynamic calculation

The basic assumption in dynamic applications is that dynamic equilibrium conditions according to the D'Alembert principle have to be satisfied at each time step. In addition to the basic equations of motion, a vector of inertial forces is introduced [5, 6]. The vector $\left\{ \boldsymbol{F}_{e,o} \right\}$ is transformed into the vector $\left\{ \boldsymbol{F}_{e,o+z} \right\}$ as follows:

$$\begin{aligned}\left\{\boldsymbol{F}_{e,o+z}\right\} &= \int\limits_{V_e}\left[\boldsymbol{V}_e\right]^{T}\left(\left\{\boldsymbol{X}\right\}-\left\{\boldsymbol{F}_z\right\}\right)\boldsymbol{dV}_e = \int\limits_{V_e}\left[\boldsymbol{V}_e\right]^{T}\left(\left\{\boldsymbol{X}\right\}-\rho\left\{\boldsymbol{u}_e\right\}\right)\boldsymbol{dV}_e = \\ &= \int\limits_{V_e}\left[\boldsymbol{V}_e\right]^{T}\left(\left\{\boldsymbol{X}\right\}-\rho\left[\boldsymbol{V}_e\right]\left\{\Delta_e\right\}\right)\boldsymbol{dV}_e = \int\limits_{V_e}\left[\boldsymbol{V}_e\right]^{T}\left\{\boldsymbol{X}\right\}\boldsymbol{dV}_e - \\ &- \int\limits_{V_e}\left[\boldsymbol{V}_e\right]^{T}\rho\left[\boldsymbol{V}_e\right]\left\{\Delta_e\right\}\boldsymbol{dV}_e = \left\{\boldsymbol{F}_{e,o}\right\}+\left\{\boldsymbol{F}_{e,in}\right\}\end{aligned} \tag{1}$$

The matrix of the mass of the whole structure has the form:

$$\left[\boldsymbol{M}\right]=\sum_{e=1}^{p}\left[\overline{\boldsymbol{M}_e}\right]=\sum_{e=1}^{p}\left[\boldsymbol{L}_e\right]^{T}\left(\int\limits_{V_e}\rho\left[\boldsymbol{V}_e\right]^{T}\left[\boldsymbol{V}_e\right]\boldsymbol{dV}_e\right)\left[\boldsymbol{L}_e\right] \tag{2}$$

Incorporating the vector $\left\{\boldsymbol{F}_{in}\right\}$ into the fundamental FEM equation results in the equation of dynamic balance:

$$\left[\boldsymbol{M}\right]\left\{\ddot{\Delta}\right\}+\left[\boldsymbol{C}\right]\left\{\dot{\Delta}\right\}+\left[\boldsymbol{K}\right]\left\{\Delta\right\}=\left\{\boldsymbol{F}\right\} \tag{3}$$

where: M - stiffness matrix,
C - dumping matrix,
K - mass matrix,
F - load vector and
Δ - vector of unknown nodal displacements.

In the case of Rayleigh attenuation, the matrix $[\mathbf{C}]$ can be expressed as consistent using the constants α and β:

$$\left[\boldsymbol{C}\right]=\alpha\left[\boldsymbol{M}\right]+\beta\left[\boldsymbol{K}\right]=0 \tag{4}$$

where: α - damping coefficient proportional to the rate of displacement and
β - damping coefficient proportional to the rate of deformation.

The mass matrix $[\mathbf{M_e}]$ is consistent. A diagonal matrix of masses concentrated into nodes is frequently used. The matrix $[\mathbf{M_e}]$ has the same internal structure as the matrix $[\mathbf{K_e}]$.

3.2 Description of used calculation software based on FEM principles

VisualFEA [7] is an innovative software application for finite element analysis, which is an advanced technique of solving and analysing physical problems arising in many fields of science and engineering. This is a full-fledged software application integrated with easy to use but powerful functions for pre- and post-processing, as well as for FE processing. VisualFEA has functions for studying the FE analysis using a deformation principle of the FEM. The various computational aspects and concepts involved in FE modelling can be easily understood through computational simulations. Its pre-processing capability includes the most advanced 2- and 3-dimensional mesh generation techniques. The FE analysis can be divided into three phases:

- • Preprocessing – these functions are used to create, edit and check the modelling data necessary for FE analysis [8]. The data are constructed in few steps such as the creation of boundary curves and primitive surfaces, mesh generation and data assignment (Boundary condition, Element property, Load condition, etc.),
- • Processing – this phase is the kernel of FE analysis. Processing does not require any user interaction and proceeds with various stages of computing element equations, assembling a system of equations, their solving, and execution of other related computations,
- • Postprocessing – functions of this group are used for the graphical visualization or further processing of the computed results to facilitate their interpretation and understanding, Fig. 3.

3.3 Description of computational models of elastic half-space

The geometric parameters of the model were based on the spatial arrangement of pipes of the longitudinal section. The investigation area was divided into interfaces depending on the geological profile; the material parameters were set to the values obtained from in-situ testing by the impulse seismic method (ISM) [6].

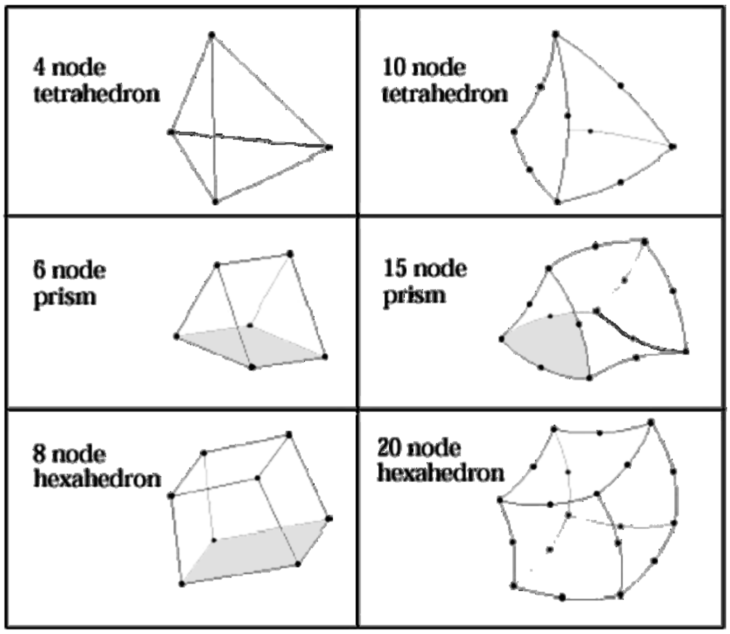

Figure 3: Implemented shape functions in VisualFEA [7].

The computational model of the subsoil was created in the VisualFEA program as a planar section shape with a circular section. The length of the trailing edge representing the ground surface was approximately 100 m and the depth was a variable ranging from 0 m to 40 m. The real geological composition in the subsoil inserted through the material constants where the elastic modulus had a value E = 40 MPa, Poisson's ratio ν = 0.33 and unit weight γ = 1900 kg.m^{-3} was used. The FEM solution resulted in a system of equations for 772 planar triangular elements interconnected by 377 points of the covered network. The mesh was generated symmetrically and was thickened and adapted close to the surface and the symmetry axis (Fig. 4).

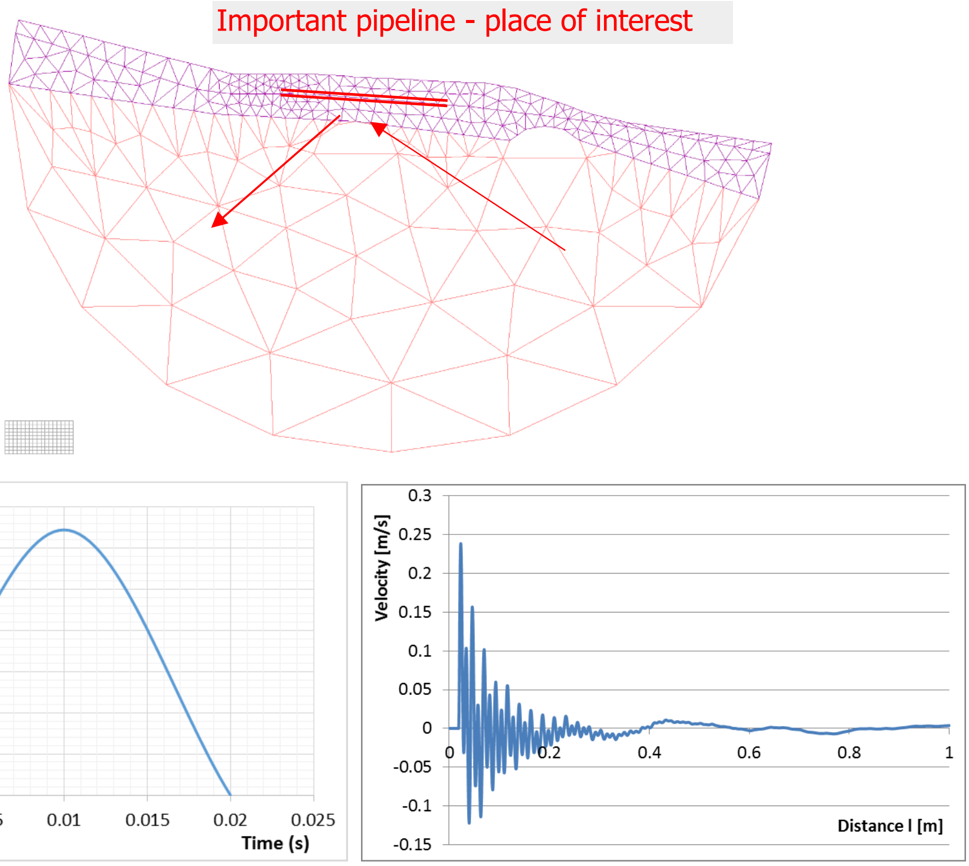

Figure 4: Subsoil model with dynamic load m_{ek} = 100 kg (up) and impulse (right) and response (left).

4 DYNAMIC PARAMETERS OF ELASTIC ENVIRONMENT - EXPERIMENT

For the requirements of numerical modelling the dynamic response of geological half-space and water pipes in the area of Žilina – Považský Chlmec and for the calibration of the dynamic interaction system (subsoil – pipeline), it was necessary to perform the dynamic diagnostics of subsoil parameters. The main objective of the dynamic diagnostics of the foundation soil in the certain geological place consisted in determining basic dynamic parameters and frequency characteristics. Considering the pursued objectives, the impulse seismic method (ISM) monitoring the process of propagating surface waves in the form of stress pulses from the source was applied. When applying the ISM, the velocity of shear (Rayleigh) (C_S, C_R) waves was measured between two accelerometers located at a set distance L on the surface of the half-space. In addition to the velocity of surface waves, the ISM can be used to determine the attenuation of the surface waves (α_R) and the transmission characteristics $Hi_{(f)}$ of the soil environment.

In this area, a series of ISM measurements was carried to determine the mentioned dynamic parameters of the soil environment, [9, 10 and 11]. The position of the impulse device and the positions of the measurement points where the accelerometers were placed are schematically shown in Fig. 4. The speed of the surface wave (C_R) was measured between the points B1 and B2. However, it was necessary to establish basic dynamic parameters to find the intensity level of the vibrations during the blasting in the studied geological locality. For the calculation of the elasticity moduli of the investigated soil environments, the following physical-mechanical properties were used: Poisson's ratio $\nu \approx 0.33$, density $\rho_{13} \approx 1\,760$ kg.m^{-3} (for top profile consisting of clays, silts and gravels), and density $\rho_{13} \approx 2\,600$ kg.m^{-3} (for rock layers).

5 RESULTS

5.1 Numerical simulation results

The result of the dynamic calculation for this variant (parametric) of the calculation model (17 variations) is shown in the graph of the distance from the blast l to the nearest point of the pipeline (maximum dynamic response) and the maximum velocity amplitude of oscillation v_{max} at this point (Fig. 5).

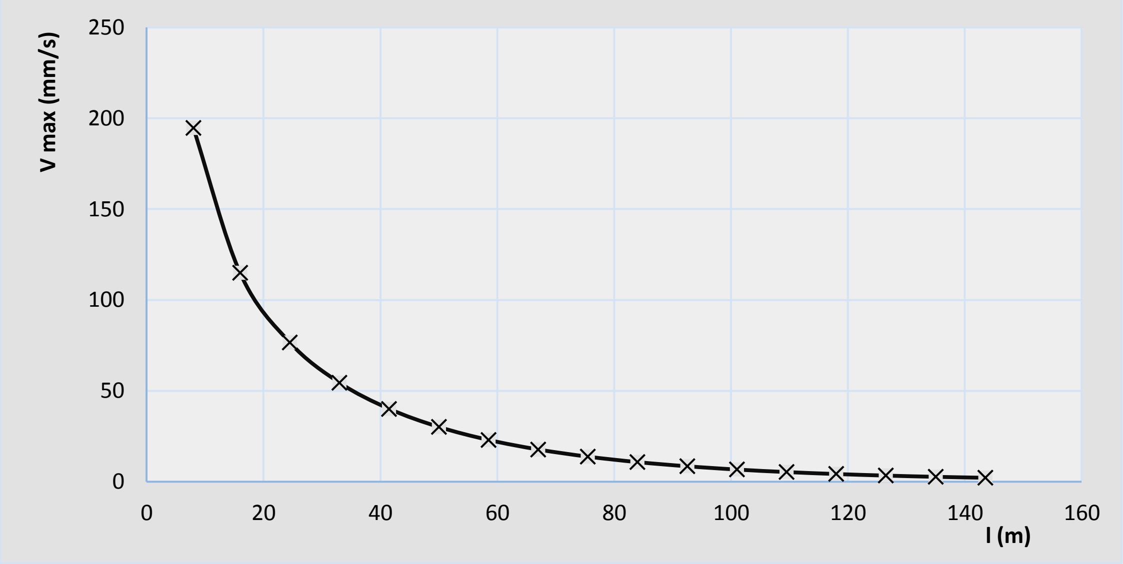

Figure 5: Results of the dynamic FEM parametric calculations of elastic environment – response at the pipeline to blasting at variable distances from the pulse caused by the explosion of intensity m_{ek} = 100 kg.

5.2 Experimental measurement results

Based on the performed correlation analysis – a mutual correlation function $R_{ik}(\tau)$, the velocities of propagation of Rayleigh surface waves were determined for the clays, silts and gravels (compacted road subsoil and sidewalks) from 0.0 to 4.0 m below the surface $C_R \approx 92 - 98\, m/s$ (impulse) and the bedrock layer from 1.0 to 5.0 meters below the surface $C_R \approx 128 - 132\, m/s$ (impulse).

Figure 6: Central part of tunnel – view on east portal.

6 CONCLUSION

Based on the experience and extrapolation of the results from the measurements of seismic effects in a sufficient quantity under approximately the same geological and geometric conditions, the following statements can be concluded. The calculation is realized in the ideal elastic and homogeneous environment whose parameters have been directly detected by the in-situ ISM method. However, geological discontinuities (or waveguides), which cannot be neglected, can cause an enormous increase in the energy transfer to the pipeline due to blasting. To assure the security of the water supply pipeline, it is necessary to monitor the dynamic response of the relevant points of the pipeline for each blast drilling in both tunnel tubes. This will make numerical modelling results reflect the real situation more accurately.

References

[1] JAKUBIS, I. 2006. Motorway D3 Žilina (Strážov) – Žilina (Brodno), km 6.850 – 11.100, part B – Tunnel Považský Chlmec. Final report. Geoconsult .

[2] DECKÝ, M., DRUSA, M., PEPUCHA, Ľ., ZGÚTOVÁ. K. *Earth Structures of Transport Constructions*. Harlow: Pearson, 2013. 180 p. ISBN 978-1-78399-925-5.

[3] KAJZAR V., DOLEŽALOVÁ H. Monitoring and Analysis of Surface Changes from Undermining. Geoscience Engineering. 2013, 59(4), 1-10.

[4] MARSCHALKO, M., YILMAZ, I., BEDNARIK, M., KUBECKA, K. *Influence of mining activity on slope deformations genesis: Doubrava Vrchovec, Doubrava Ujala and Stařič case studies from the Czech Republic. Engineering Geology*. 2012, 147, 37-51.

[5] PERSSON P. A., HOLMBERG R., LEE J. *Rock Blasting and Explosives Engineering*. Boca Raton, Fla.: CRC Press, 1993. 560 p. ISBN 0-8493-8978-X.

[6] BENČAT, J., STYPULA, K. Buildings structure response due to railway traffic. In: Communications: scientific letters of the University of Žilina. - ISSN 1335-4205. - Vol. 15, no. 2 (2013), 41-48. (Civil-Comp Proceedings, 102. - ISSN 1759-3433).

[7] VisualFEA, available from: http://www.visualfea.com/introduction.htm [Cit. 10/2015].

[8] KORTIŠ, J. The stress analysis of the industrial fiber-reinforced concrete slab on elastic subgrade loaded by the operational loading. In: *Applied Mechanics and Materials*. 2014, 617, 46-49.

[9] FIGULI, L. MAGURA, M. KAVICKÝ, V. JANGL, Š. Application of recyclable materials for an increase in building safety against the explosion of an improvised explosive device. In: *Advanced Materials Research*. 2014, 1001, 447-452.

[10] KUCHÁROVÁ, J. MELCER. J. 2004. Experimental investigation of rubber pads under dynamic load. In modelling and optimisation in materials science, MOK '43, April 22-23, 2004, Odessa. Astroprint. 2004. ISBN 966-318-117-6, 187-189.

[11] VANĚK M., TOMÁŠKOVÁ Y., STRAKOVÁ A., ŠPAKOVSKÁ K., BORA P. Risk Assessment in Mining-Related Project Management. *Geoscience Engineering*. 2013, 59(3), 47-53.